Progress in Additive Manufacturing (2021) 6:243–256
https://doi.org/10.1007/s40964-020-00158-y

FULL RESEARCH ARTICLE

I-support soft arm for assistance tasks: a new manufacturing approach based on 3D printing and characterization

Luca Arleo[1,2] · Gianni Stano[3] · Gianluca Percoco[3] · Matteo Cianchetti[1,2]

Received: 7 July 2020 / Accepted: 7 November 2020 / Published online: 22 November 2020

Abstract
Soft robotics is an emerging scientific field well known for being widespread employed in several applications where dexterity and safe interaction are of major importance. In particular, a very challenging scenario in which it is involved concerns biomedical field. In the last few years, several soft robotic devices have been developed to assist elderly people in daily tasks. In this paper, the authors present a new manufacturing approach for the fabrication of I-SUPPORT, a soft arm used to help needful people during shower activities. The proposed I-SUPPORT version, based on pneumatic and cable-driven actuation, is manufactured using Fused Filament Fabrication (FFF), the most common and inexpensive Additive Manufacturing (AM) technology. The advantages offered by FFF technology compared to traditional manufacturing methods regard: (i) the possibility to increase the automation degree of the process by reducing manual tasks, (ii) the decrease of assembly operations and (iii) an improvement in terms of supply chain. Moreover, the constitutive I-SUPPORT elements have been printed separately to save time, reduce materials and optimize the waste in case of failure. Afterwards, the proposed soft robotic arm has been tested to evaluate the performances and of the chambers, module and the whole I-SUPPORT manipulator.

Keywords Additive manufacturing · Fused filament fabrication · Soft actuator: soft assistive robot · Flexible filament · Airtight

1 Introduction

Additive manufacturing (AM) is an emerging manufacturing approach composed by 7 process groups [1], but the general manufacturing idea underlying all the groups is the same: fabricate objects layer by layer. The AM application fields are many, ranging from the aerospace one [2–4] to electronic fields [5–9], but at the state of art, Additive Manufacturing (AM) is still underexploited in the soft robotic field. This new engineering discipline is characterized by several and complex features, the main ones are: the usage of soft materials (with a Young modulus lower than 10^9 Pa) or compliant structures, the high bio-inspiration degree, the usage of several actuation methods (including non-conventional ones) and the possibility to modulate the stiffness of body parts [10–14]. The most common technique used to fabricate soft devices is moulding, in all its variants (e.g., vacuum casting or multi-step moulding). In authors' opinion, AM technologies aimed to the manufacturing of soft robots will result in several advantages, as explained in more detail some lines below. The possibility to use AM technologies to manufacture very complex geometries (difficult to fabricate using traditional manufacturing approaches such as elastomeric materials moulding), to better mimic animal and vegetable shapes and movements [12] is very attractive and challenging. A clear example of the close link among AM and soft robotic is represented by the Bionic Handling Assistance (BHA) developed by Festo Inc. using Selective Laser Sintering (SLS) technology [15]. In the last few years the number of soft robots manufactured with AM technologies grew up considerably [16], several AM technologies have been exploited to fabricate soft manipulators, such as

✉ Gianluca Percoco
gianluca.percoco@poliba.it

1 Scuola Superiore Sant'Anna, The BioRobotics Institute, Viale Rinaldo Piaggio 34, Pontedera, 56025 Pisa, Italy

2 Department of Excellence in Robotics & AI, Scuola Superiore Sant'Anna, Piazza Martiri della Libertà 33, 56127 Pisa, Italy

3 Department of Mechanics, Mathematics and Management, Polytechnic University of Bari, Via E. Orabona 4, 70125 Bari, Italy

Fused Filament Fabrication (FFF) [17, 18] and Digital Light Processing (DLP) [19, 20].

In the field of assistive soft robotics, Manti et al. developed an innovative robotic system to help non-autonomous elderly people during bathing tasks within the EU funded I-SUPPORT project [21, 22]. I-SUPPORT is a soft robotic arm that can be safely used to reach target areas of the human body to assist needful people in taking shower. It is based on a hybrid actuation system: a McKibben-based flexible fluidic actuation system and a cable-driven system that are combined to achieve complex movements in the 3D space. I-SUPPORT is a modular manipulator made up of three assembled modules: the first one is called proximal module and is actuated only by cable-driven system to compensate gravitational effects; the second and third modules are called, respectively, central and distal module both based on the same hybrid actuation (cable driven and fluidic actuations).

Each module is composed of three McKibben pneumatic actuators positioned at 120° around a circle with a radius equal to 3 cm, and three cables. The manufacturing steps underlying pneumatic chambers fabrication are reported in [21], but here we recall the main components to underline the advantage of the proposed approach:

1. a braided sheath (Pro Power PETBK3B10, Farnell Components) is expanded and inserted into a metallic cylinder and thanks to a mechanical deformation and a thermal treatment a permanent cylindrical bellow shape is created;
2. a balloon of latex is introduced into the braided sheath to create the internal chamber;
3. both extremities are sealed by means of two end-caps, one needful to house the air connector and the other used as anchoring point.

After the pneumatic chambers are manufactured, they are arranged around a circular base and several custom-made helicoidally shaped supports are placed among the chambers to house the cables.

The whole manufacturing process underlying I-SUPPORT is multi-phase and it requires several manual assembly steps and different components such as braided sheath, balloon, air connector, end-caps and supports.

In this paper it is shown that the fabrication of a re-engineered version of the I-SUPPORT device is possible using an AM approach: the proposed I-SUPPORT version manufactured through Additive Manufacture is called "AM I-SUPPORT".

Fused Filament Fabrication (FFF) technology, well known for being one of the most common and inexpensive AM technology, and two commercial filaments have been employed. More in detail, the use of FFF in manufacturing the soft assistive manipulator brings several advantages, such as: (i) most assembly operation are avoided by manufacturing more components in a single-step printing cycle since the pneumatic chambers are equipped with embedded air connectors, (ii) the manual tasks are reduced, (iii) from a supply chain point of view only two commercial filaments are required to produce the whole device, (iv) repeatable results have been obtained fabricating identical pneumatic chambers with separate cycles.

Finally, the whole AM I-SUPPORT has been tested to characterize its behaviour in terms of bending capabilities and covered workspace.

Although this approach is validated on a specific soft robotic arm, we believe that the reported results can be a useful example of advantages introduced by AM in fabricating soft robotic arms in general, thus widening the interest and the impact of the proposed methodology.

2 Materials and methods

2.1 AM I-support design

AM I-SUPPORT has been re-engineered maintaining modularity with two identical modules, called proximal and distal module, connected each other to obtain complex movements. As well as in the previous version, every AM I-SUPPORT module is equipped by air connectors and cable seats to combine pneumatic and cable-driven actuation: while pneumatic chambers are inflated by means of compressed air to obtain several manipulator movements, cables are pulled via DC motors to provide an antagonistic action to the fluidic actuators that results in a stiffening of the modules.

As shown in Fig. 1, each AM I-SUPPORT module is composed of the following elements: (i) three pneumatic chambers arranged with an angular distance equal to 120° and with embedded air connectors and (ii) two (bottom and top) terminals named, respectively, end plate and base plate, that allow direct and fast connections, both between the two modules and between external elements as support frame and (iii) six rings arranged along the actuator chambers to keep the correct working position and to house the cables.

Furthermore, commercial nuts and bolts have been used to assemble all the components and finally the cables were placed in appropriate seats to provide the cable-driven actuation. The size of the single module (see Fig. 1) is 60×202 mm, while overall weight is 183 g.

The main innovative aspect of the AM I-SUPPORT concerns the elimination of the manual steps in assembling the actuators and in coupling pneumatic chambers with air connectors, as a matter of fact the pneumatic chambers have been manufactured with embedded air connectors in the same single-step printing cycle. The embedded air

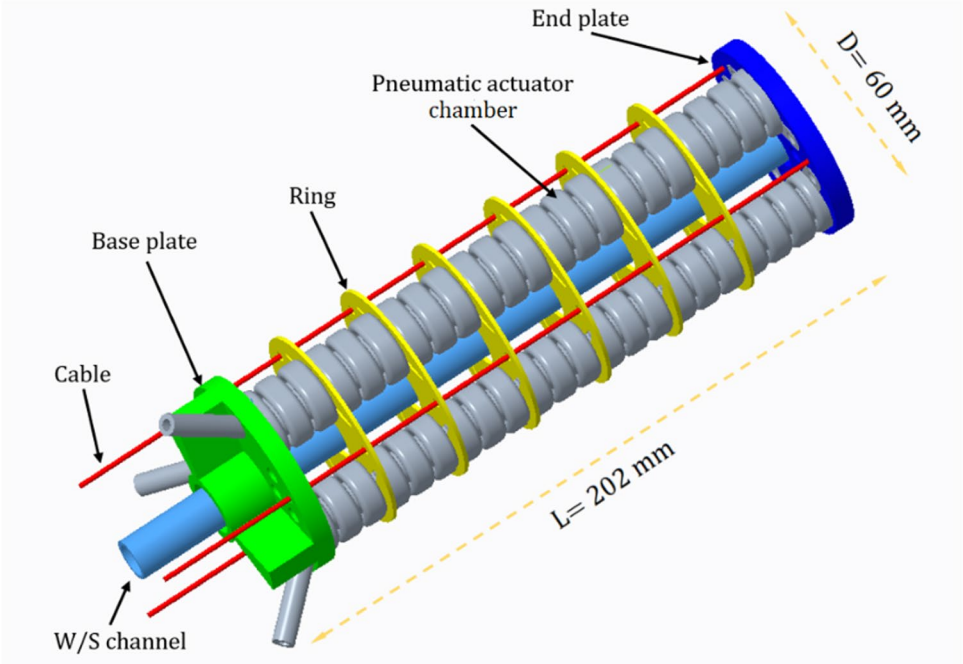

Fig. 1 CAD design of the AM I-SUPPORT single module

connectors ensure airtightness at the interface between pneumatic chambers and pneumatic pipe.

Pneumatic chambers have been designed using the same shape as I-SUPPORT: a bellows-like shape to obtain huge deformations; in Fig. 2, the design of the chambers and internal micro-chambers is reported. The new actuator chambers have been designed following Design for Additive Manufacturing (DfAM) approach, a collection of techniques based on the idea that design optimization is crucial to take more advantages from AM technologies [23–25].

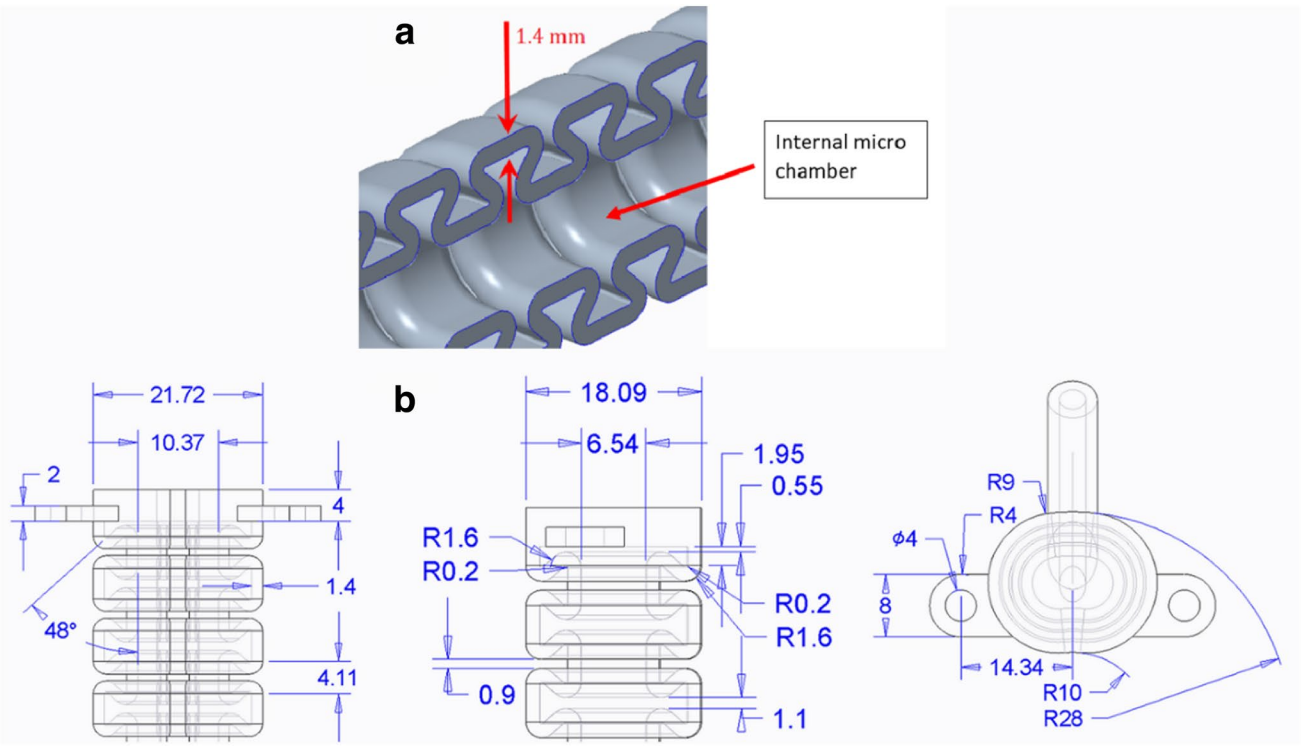

Fig. 2 Actuator pneumatic chamber **a** cross section of the actuator chamber; **b** dimensions in mm of the micro-chambers

When objects that will be 3D printed are designed, several considerations concerning the AM process must be considered (such as printing orientation, supports utilization, printing parameters to set, materials to use etc.…) to obtain improved manufacturing results:

(i) The internal micro-chambers have been designed and manufactured (see Fig. 4), to avoid irremovable supports inside the chambers.
(ii) Pneumatic chambers have been fabricated using a nozzle diameter equal to 0.4 mm, and particular attention has been payed to the *Line width* parameter that affects the width of the extruded filament (see Fig. 3) and consequently affects the total number of adjacent extruded lines deposited by nozzle on each slice.
(iii) After setting the extrusion width to 0.4 mm, equal to the nozzle diameter, using a trial-and-error approach, it has been found that, under specific conditions, the lower wall thickness of the chamber ensuring air tightness and the flexibility required by the application is 1.4 mm. So, the wall thickness of the pneumatic chambers (see Fig. 2a) depends both on extrusion width parameters and on further parameters affecting air tightness, as discussed in Sect. 2.2.

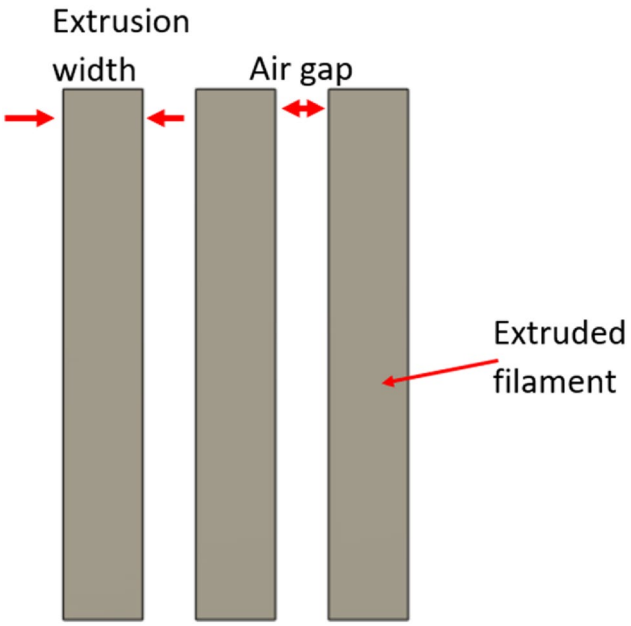

Fig. 3 Line width and air gap parameter

Table 1 Printing process parameters

Process parameters	Actuator chambers	Rings	Terminals
Material	TPU 80A	TPU 80A	PLA
Printing speed (mm/s)	20	20	80
Layer height (mm)	0.1	0.15	0.25
Extrusion width (mm)	0.4	0.4	0.5
Wall line count	2	5	2
Infill density (%)	100	100	15
Infill pattern	Concentric	Lines	Grid
Printing temperature (°C)	235	235	205
Heated bed temperature (°C)	60	60	40
Flow (%)	105	105	100
Printing time (hours)	60 (20 for each one)	3.2	3.5

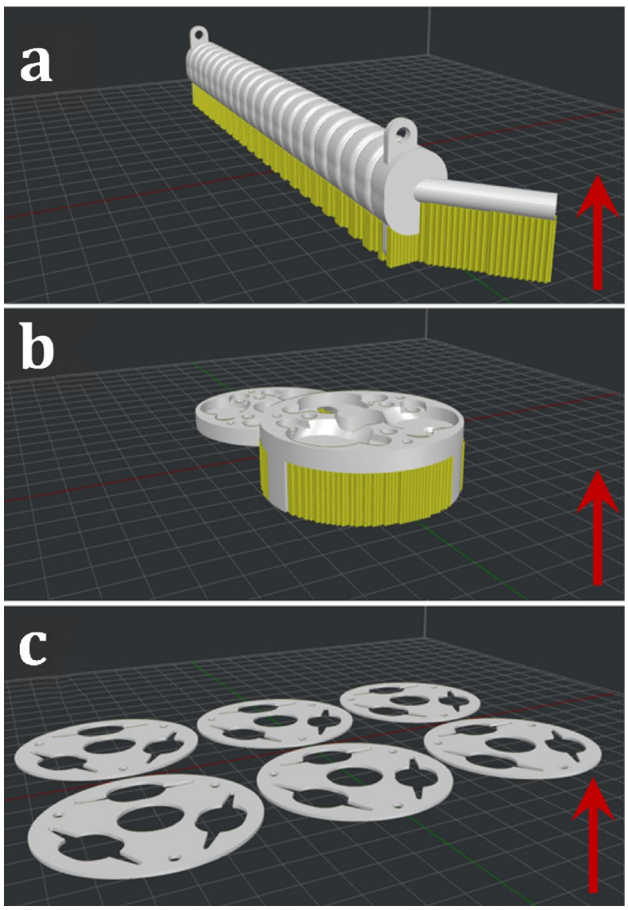

Fig. 4 3 constitutive components of AM I-SUPPORT in slicing software (the red arrow indicates the building direction): **a** actuator chambers, **b** terminals and **c** rings (in white constitutive material, in yellow supports)

2.2 AM I-support manufacturing

The Raise3D Pro2 3D printer has been employed in this study. It is a dual-extruder FFF printer with a direct extrusion system, most suitable for the printing of soft filaments than its counterpart (bowden-based machine). The slicing software used to communicate with the 3D printer was Idea Maker 3.4.3. Two commercial materials have been chosen to create the manipulator: (i) actuator chambers (equipped with embedded air connectors) and rings have been fabricated using a thermoplastic polyurethane with Shore A hardness equal to 80 (TPU 80A LF), by BASF™; (ii) the terminals have been manufactured in polylactic acid (PLA), by Raise3D™.

The TPU 80A LF is characterized by a tensile modulus of 17 MPa and elongation at break of 471%, for accommodating the huge deformations expected on the chambers. On the other hand, PLA is a harder material with a tensile modulus of 2.6 GPa. It has been chosen to print the two terminals with a low value (15%) of infill density without sacrificing neither stiffness nor light weight. All the materials data come from their respective technical data sheet.

Despite the 3D printer ensures the possibility to simultaneously use two materials, with the theoretical possibility to print the whole manipulator in a single-step printing cycle, printing each I-SUPPORT element separately has been preferred, due to the following considerations: (i) to avoid issues related to multi-material printing (for instance cross-contamination or low materials affinity) [26–28]; (ii) to minimize both the material usage and printing time; (iii) to reduce waste in case of errors; and (iv) to keep the possibility to replace single elements with spare parts instead of the whole module.

In Table 1, the printing parameters set for each component are shown. Another advantage related to the separate manufacturing consists in the possibility to create different printing configurations, including printing parameters and orientation (see Fig. 4), for each component. Each component has been fabricated with a 0.4 mm nozzle.

One of the most important requirements for the actuator chambers is air tightness, especially when relatively high pressure values (4 bar in this case) are required. In authors' opinion AM of airtight structures is a challenging and attractive topic itself with the potential of increasing the contribution of AM processes in the soft robotics field. Previous studies point out that the printing parameters affecting tensile strength of FFF components are: layer height, extrusion width, printing temperature and air gap [29–32]. The tensile strength of the pneumatic chambers must be increased to avoid any possible breakages (which involves air leakage) when a pressure of 4 bar is reached. Low values of layer height and extrusion width, respectively, 0.1 mm and 0.4 mm (the same value of the used nozzle diameter) and temperature values higher then suggested by supplier, namely 235 °C instead of 225/230 °C have been set to improve interlayer adhesion and consequently the tensile strength.

Air gap, defined as the space among two adjacent extruded lines of filament (see Fig. 3), is a further parameter affecting air tightness. If the air gap value is positive, there is a distance between adjacent lines, if it is negative there is an overlap between adjacent lines. As demonstrated in [29], the lower air gap is, the higher the tensile strength, so we have set the parameter "maximum shells overlap percentage" as 50% to achieve a negative air gap.

By printing separately each component, the total printing time, computed as the sum of printing time of each component, is less than the printing time required by the AM I-SUPPORT module in a single and non-stop printing cycle (about 66.7 h in the first case against 120 h for the second one) for a cost estimation of 19.4 €. The manufacturing choice of a separate printing involves a time reduction because of the support optimization: in this way the required supports are less than in the other case resulting in a reduction of used materials and, therefore, saving time. Moreover, the advantage of reduced waste in case of printing failure has been considered.

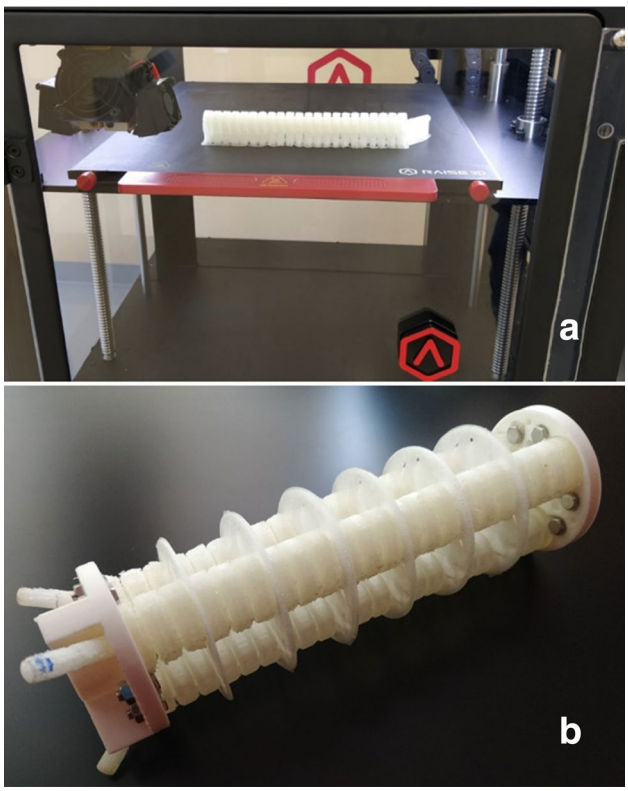

Fig. 5 **a** Manufactured soft actuator chamber in 3D printer; **b** assembled module

In Fig. 4, printing orientation for each I-SUPPORT component is shown, highlighting in yellow the required external supports. Figure 5 shows the actuator chamber after the manufacturing process, into the 3D printed build construction room, and the assembled module made up of three pneumatic chambers, terminals and rings. The components have been assembled with the same cables used in the I-SUPPORT soft robotic arm.

3 Characterization tests

In this section, the characterization tests performed to understand the behavior of (i) the single pneumatic chamber, (ii) the single module and (iii) the whole manipulator are reported. For greater clarity, it has been decided to separately describe the measurement protocols and setup used for the characterization (in Sect. 3) and the respective results and comparison between the two versions of the manipulator (in Sect. 4).

3.1 Pneumatic chambers elongation

As regards the pneumatic chambers, the dependence of elongation on the pressure input and repeatability over the chambers have been investigated. The measurement setup consisted of (i) an air compressor (Hyundai KWU750, Pmax 8 bar); (ii) a rigid frame to which the chamber was fixed by means of a 3D printed customized PLA support, equipped with a square millimeter grid; and (iii) a Canon EOS D400 digital camera to capture the elongation.

To avoid the Mullins effect impact during experimental test, once printed and treated to remove supports, all chambers have undergone the same load–unload cycle under growing pressure inputs up to 4 bar before testing.

Six chambers have been tested as follows: starting from 0 bar the pressure has been increased, step by step, with 0.5 bar steps, up to 4 bar. At each step one image has been captured to compute the related elongation (ΔL) of the chamber (Fig. 6). The mean elongation value (μ), for each pressure input of the six chambers and the error bars have been calculated.

3.2 Single modules elongation and bending

After pneumatic chambers characterization, three different modules have been assembled and tested to quantify: (i) single module elongation and variability and (ii) single module bending and variability between the three modules.

To evaluate the elongation, the three pneumatic chambers that make up the single module have been pressurized at the same time and with identical pressure input. The measurement protocol is the same used for

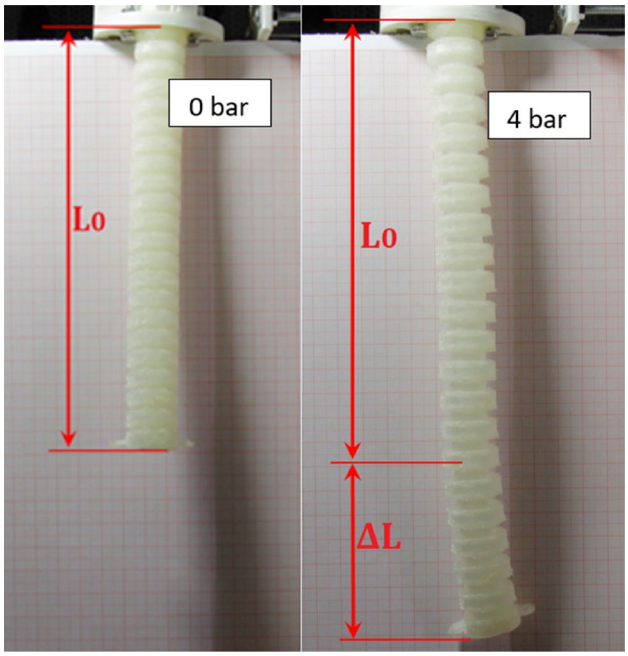

Fig. 6 Pneumatic chamber elongation

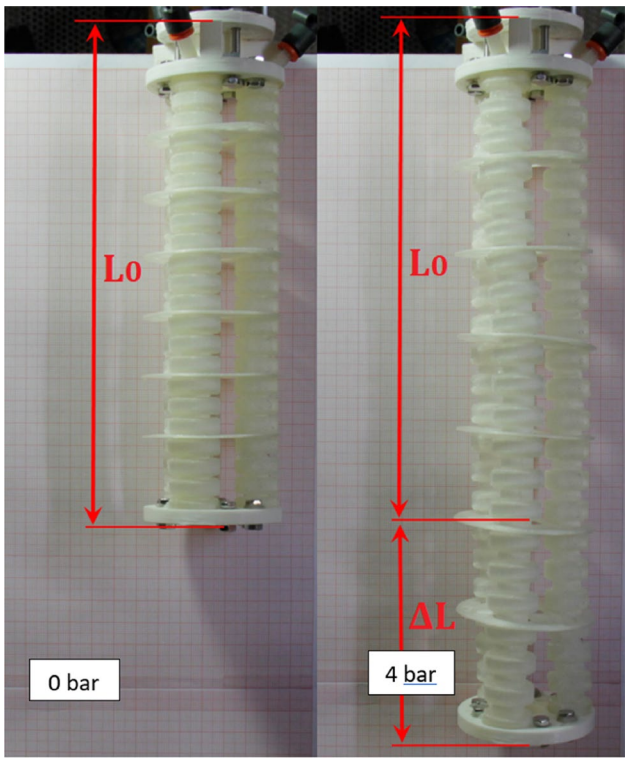

Fig. 7 Module elongation

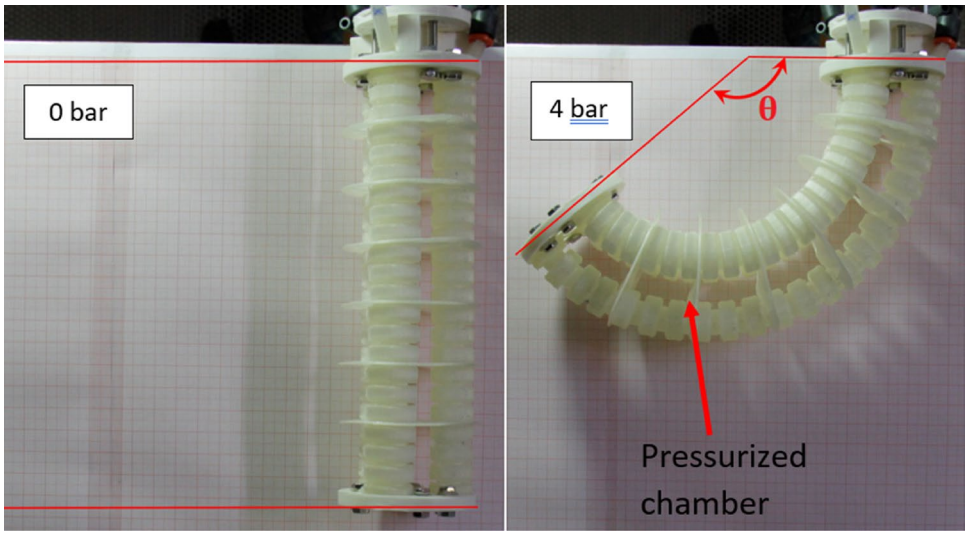

Fig. 8 Module bending

the characterization of the pneumatic chambers. Figure 7 shows how the elongation of the module has been calculated.

Finally, the bending capability of the three modules has been quantified by calculating the bending angle θ, as shown in Fig. 8. To obtain bending movement of the module, only one pneumatic chamber has been inflated, while the other two were left unpressurized.

3.3 Manipulator performance

Two modules have been connected each other using nuts and bolts to obtain more complex movements of the whole manipulator and to evaluate its workspace. Several tests have been performed on the assembled manipulator using the experimental setup reported in Fig. 9. The proximal module was fixed to a custom made 5 mm thick Plexiglass frame. Since the AM I-SUPPORT is conceptually equivalent to the previous version, the same control system developed for the latter was used, changing only some elements of the pressure input system. The control system allows to set the pressure value of actuator chambers by controlling six proportional pressure regulator valves (Camozzi, K8P-0-D522-0) to modulate separately for each actuator the input pressure supplied by the compressor (Junior 30 Werther international S.p.A.) settled at 6 bar. Moreover, the control system allows to change the cable stroke, in a range between + 200 mm (pull) and − 450 mm (release) with respect to the rest position, by controlling six servomotors (Hitec HS-785HB) at which cables have been connected. A USB interface and a purpose-built Matlab code were used to communicate with the manipulator. Figure 10 shows the labels assigned to each actuator chamber and cable.

Several tests have been performed to assess the manipulator performances. The tests have been performed using both pneumatic and cable-driven actuation in separate and combined configuration, then the displacement have been measured as explained in Sect. 3.1.

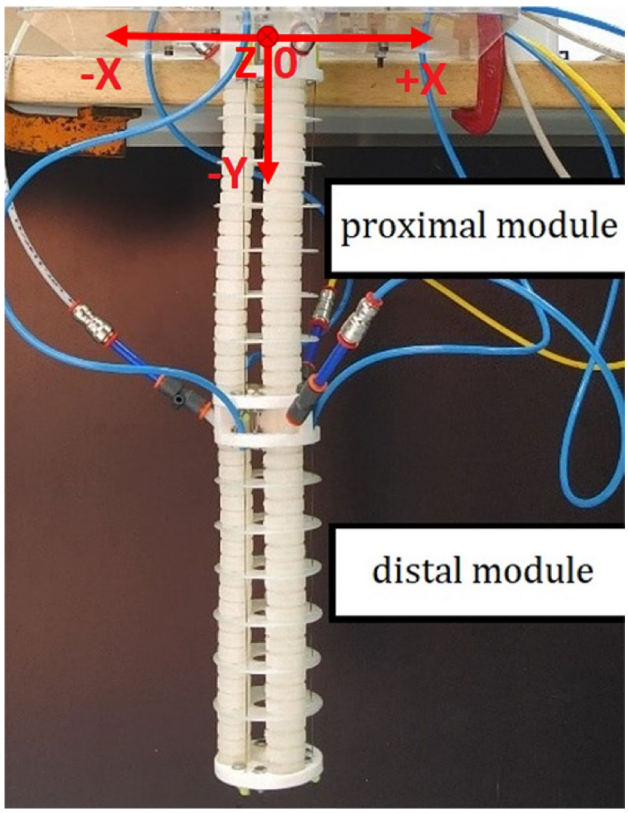

Fig. 9 Manipulator configuration used for characterization tests

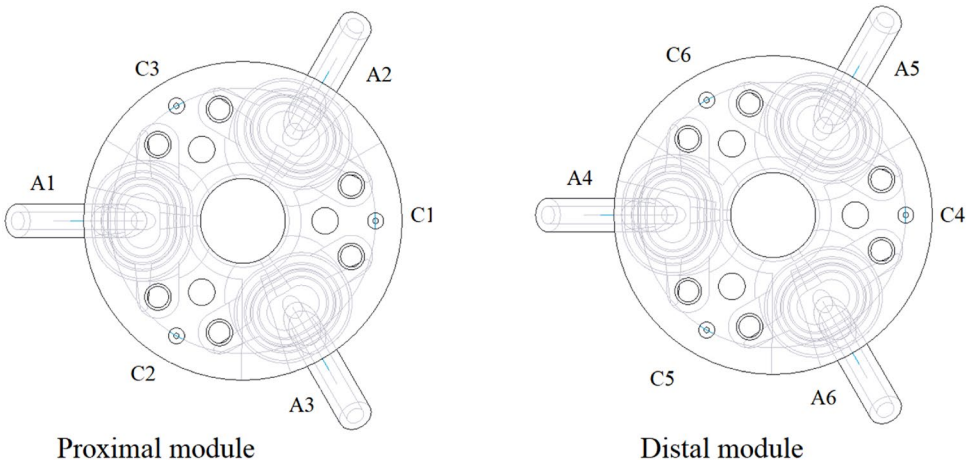

Fig. 10 Labels assigned to pneumatic chambers and cable seats

3.4 Elongation and bending of distal and proximal module

At first, the manipulator overall elongation has been evaluated activating all chambers of the two modules at the same pressure input. Subsequently, the bending performances of the two modules have evaluated separately in terms of bending angle. While the distal module has been activated by means of the fluidic actuation only, in the proximal module activation both fluidic and cable-driven actuation have been used. The activation protocol follows:

- Pattern 1: Activation of all actuator chambers (A1:A6) at the pressure input from 0 to 4 bar, without cable actuation, to obtain elongation of the whole manipulator.
- Pattern 2: Activation of a single actuator chamber (A4) at the pressure input from 0 to 4 bar, without cable actuation, to obtain bending of distal module.
- Pattern 3: Activation of a single actuator chamber (A1) at the pressure input of 2 bar, with activation of the cable in entirely opposite position (C1), to obtain bending of proximal module.

3.5 Bending of the distal module in the principal planes

Finally, keeping the proximal module at rest position, the distal module bending performances have been evaluated in the three principal planes. The activation protocol follows:

- Pattern 4–6: Activation of the pneumatic chambers useful to obtain counterclockwise bend in the principal planes (A4, A4-A5, A4-A6) at the same pressure input from zero to 4 bar.
- Pattern 7–9: Activation of the pneumatic chambers useful to obtain clockwise bend in the principal planes (A5-A6, A6, A5) at the same pressure input from zero to 4 bar.

4 Results and discussion

4.1 Pneumatic chambers elongation

The mean elongation value of the six chambers at each pressure input is reported in Fig. 11 together with error bars. The maximum variability (σ) value of 23.5 mm occurs when the maximum pressure of 4 bar is reached, although the μ/σ ratio increases when the provided pressure increases too. This behavior depends on manufacturing disturbances such as vibrations, room conditions, filament conditions and highlights that the lower the working pressures are, the more repeatable the performances of the chambers.

The percentage value of elongation of the chambers is quite remarkable (> 40%). This value demonstrates that elongation can be easily achieved by local deformation (deployment) instead of global stretching of the fluidic chamber wall, making harder materials still suitable for the purpose. It also important to underline that neither failures nor leakages have been reported during all the tests, confirming that validity of the approach used to fabricate the fluidic chambers and the embedded connectors.

4.2 Single modules elongation and bending

Data on elongation as a function of the pressure input for each module, mean elongation value of the three modules (μ) for each pressure input and the relative error bars are shown in Fig. 12a. As already observed in the case of the single pneumatic chambers, also the three modules are characterized by a certain variability which increases when supplied pressure increases. The deviation, under the same pressure input, is smaller compared to the result obtained on single chambers, probably because the usage of three different pneumatic chambers reduces meaningfully the variability. While for chambers characterization the deviation becomes significant when pressure values greater than 2 bar

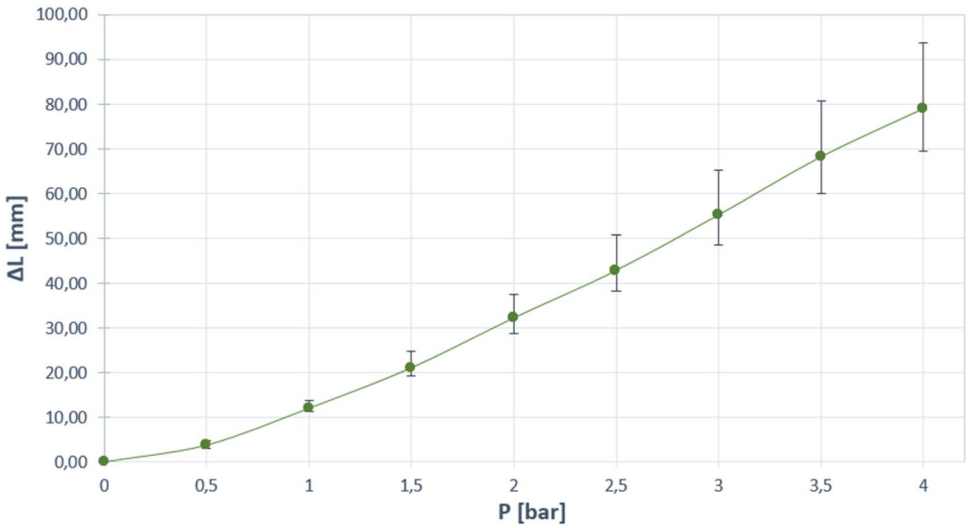

Fig. 11 Mean elongation value with error bars of the six chambers at each pressure input

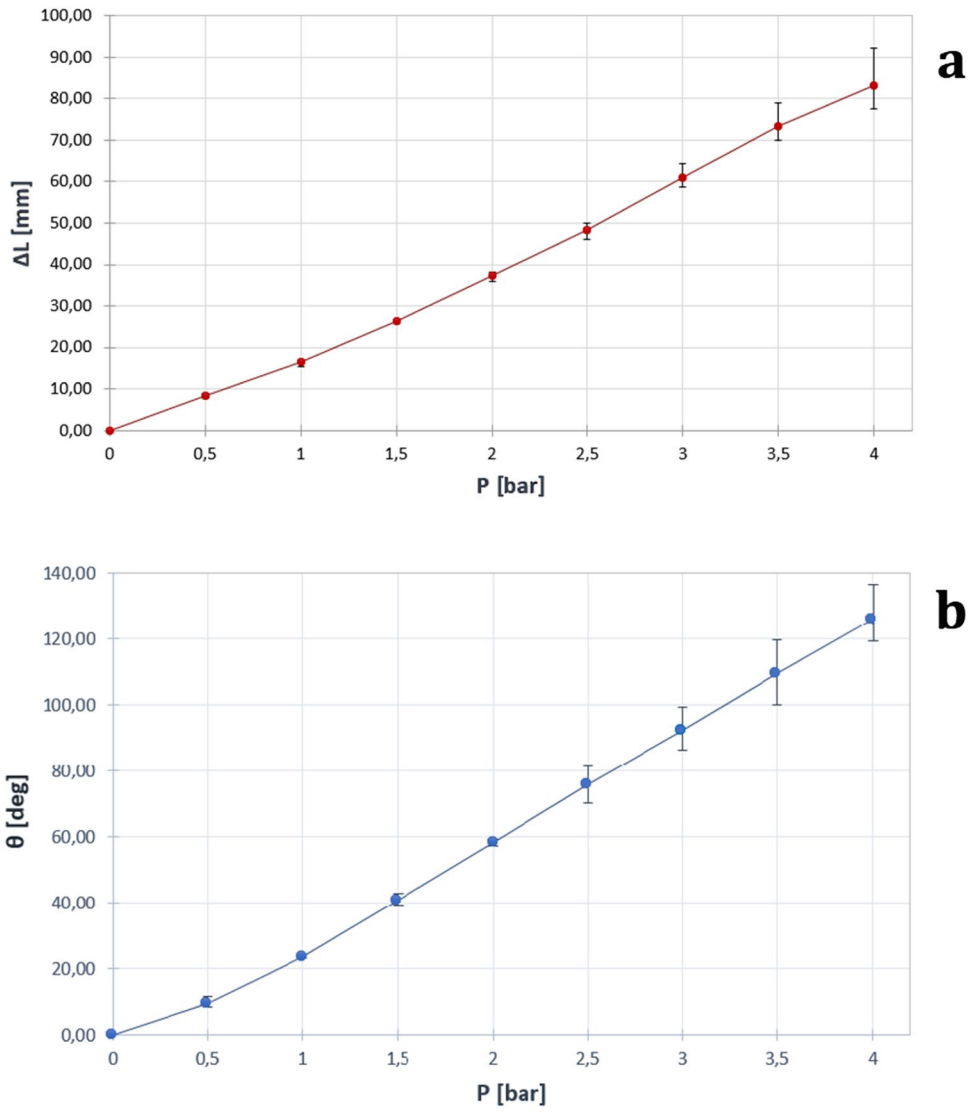

Fig. 12 **a** Mean elongation value with error bars of the three modules at each pressure input; **b** Mean bending angle value with error bars of the three modules at each pressure input

were reached, in this case it happens only when the pressure is greater than 3 bar.

The same kind of trend is visible also on bending tests. The experimental results shown in Fig. 12b highlight that there is variability among the three modules, and it increases, as well as for the elongation characterization of chambers and modules, when the supplied pressure increases. In particular, the deviation takes significant values when pressure higher than 2, 5 bar are reached.

Module elongation values are in line with the performances reported for single actuators. This was somehow expected, but cross interferences between the three chambers elongations could not be excluded a priori. The transversal rings, in fact, are coupling the deformations of the three fluidic chambers and a non-homogenous elongation of one of them may have affected also the others. The effect is very limited and shown in the next section (about overall manipulator evaluation) as out-of-axis elongation. Moreover, the number and placement of the rings demonstrated to be correct, since no inter-ring bulging have been experienced during operation.

Module bending reaches remarkably high values, in line with expectations for the development of a soft arm for assistive tasks. The precision obtained through the use of AM also results in higher symmetry of the used geometries that affects the overall performances. This is also visible in the curvature of the single module (Fig. 8), which is smooth and continuous and very close to a perfect arc of circumference. This feature, together with the linear relation between pressure and elongation, represents an important factor for future works on motion control of the soft arm.

4.3 Manipulator performance

The whole manipulator has been assembled and the activation protocol reported in Sect. 3.3 has been implemented to evaluate elongation and bending.

Pattern 1 tests shown elongation in line with expectation. The results reported in Fig. 13a show that the inflation of all the six chambers (both modules) at maximum pressure (4 bar) results in an elongation that is the double observed with single modules. Each module has a very similar behavior, but also present a slight out-of-axis deformation, which linearly increase the manipulator tip deviation along y-direction up to a maximum of $\cong 4$ mm as shown. At module level, it is not remarkable, but these out-of-axis contributions sum up and may lead to a more visible overall deviation.

Differently from the tests reported in the previous section, bending tests here focus on the evaluation of the effect of the presence of the distal module on the performance of proximal module and vice versa.

Pattern 2 aims at evaluating the relationship between pressure values of activated chambers (A4) and angle of bending of distal module. The results can be linearly approximated and at 4 bar the value of the bending angle is 137 , as shown in Fig. 13b. In this case, bending performance is not particularly affected by the presence of the proximal module (bending values are comparable), but its activation changes the center of gravity of the arm, so that the module results in a different spatial position and orientation in the global reference system. For practical use, this effect can be minimized by activating the actuators of the proximal module that act antagonistically.

Pattern 2 is resulting from the preliminary observation of the effect of the weight of the distal module on the proximal one. Fluidic actuators only are not able to stably sustain the moment generated by the distal module when the pressure exceeds 2 bar. In this case, with the combination of fluidic and cable-driven actuators, it is possible to obtain remarkable bending angles, in line or (in principle) even greater than the angles obtainable with separate actuation. Results reported in Fig. 13c show that 2 bar of inflation in chamber (A1) and the opposite servomotor activated to achieve a stroke on the cable of 175 mm lead to a bending of almost 105 deg transferred to the distal module.

Finally, the bending capability of the distal module has been tests in all principal bending planes. The terminal (end plate) trajectory of the activated module is reported in Fig. 14. The results show that the behavior of the manipulator varies if different patterns are considered, but also that deviations in the three principal bending planes are generally low.

4.4 I-support vs AM I-support

By comparing the AM I-support with the previous version, it is possible to see how the manufacturing process affects all the aspects of interest in the evaluation of the manipulator from an overall point of view. In Table 2, different aspects related to both manufacturing process and performances of single modules are listed.

It is important to note that all the parameters imposed by the scenario remained unchanged or very similar. This is particularly important for the size, the weight, which should remain compatible with the intended task. Some disadvantages are related to a slightly higher production cost, a reduced elongation capability and a higher input pressure required for operating. Shortening is also not possible, but the main use of the cable-driven actuation is more related to its antagonistic action for stiffening. On the other side, the AM I-SUPPORT represents an improvement for the high automation degree of the manufacturing process that reduces number of parts to be assembled, improves repeatability and also affects manufacturing time. Moreover, taking into account only pneumatic actuation, the bending capabilities are enhanced.

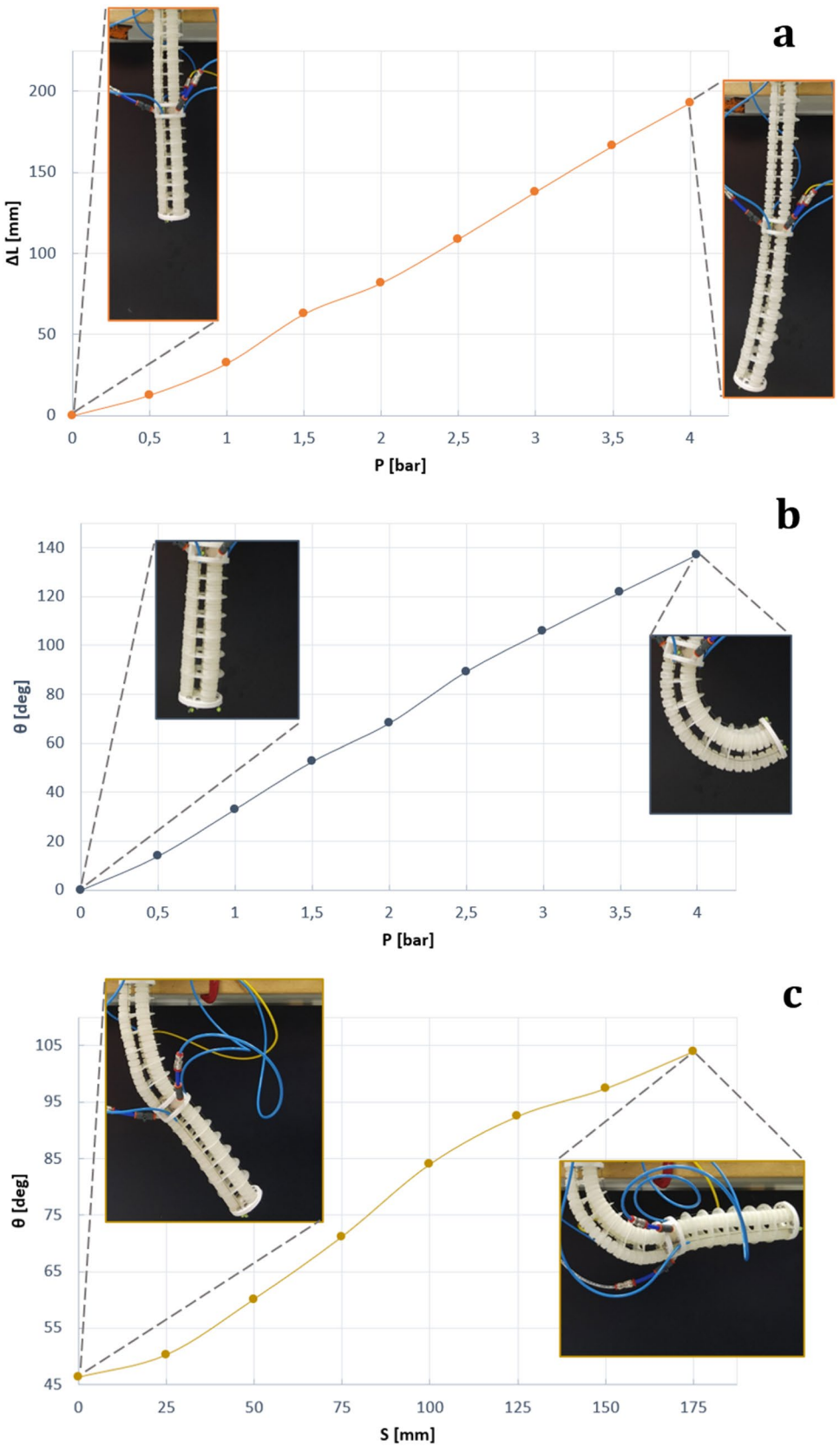

Fig. 13 **a** Elongation of whole manipulator (pattern 1); **b** bending of distal module (pattern 2); **c** bending of proximal module (pattern 3)

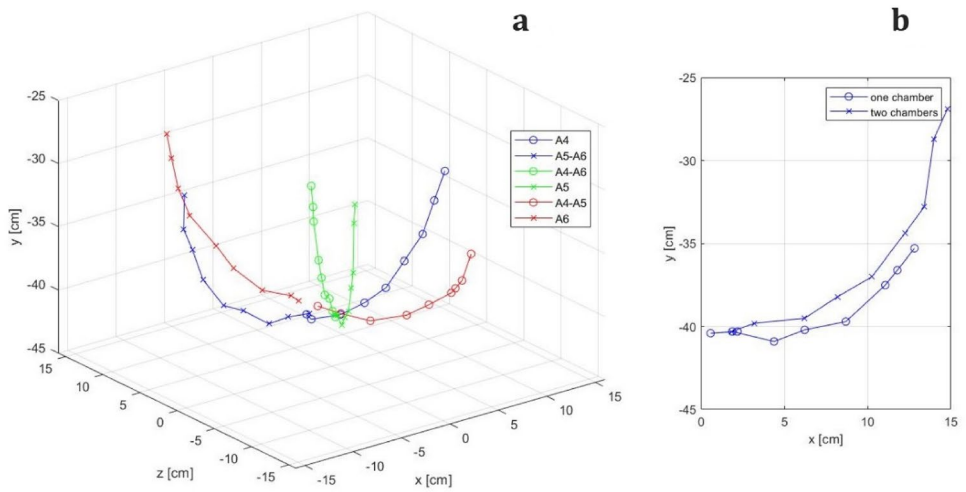

Fig. 14 **a** Bending of the distal module and relative activation patterns 4–9. **b** Bending capabilities of one or two activated chambers reported on the same plane for direct comparison. Points refer to tip position and the zero reference point, as shown in Fig. 9, is coincident to the intersection between the central axis of the manipulator and the plexiglass frame

Table 2 Comparison between the two versions of the manipulator

	I-SUPPORT	AM I-SUPPORT
Dimensions	205 × 60mm	202 × 60 mm
Weight	180 g	183 g
Cost (material consumption)	15 €	19.4 €
Required material	Braided sheath Balloon Actuator terminals Nuts and bolts Cables Helicoidal structure Plexiglass rigid terminals Custom-made interface for Module connection	TPU 80A filament PLA filament Nuts and bolts Cables
Supply chain network	Many suppliers	Few suppliers
Machine manufacturing time	Unknown	66.7 h
Assembly manufacturing time	8 h	1 h
Automation degree of the manufacturing process	Low	Improved
Pressure inputs range	0–1.2 bar	0–4 bar
Elongation (ΔLmax/L0)	+72%	+47.6%
Shortening	Allowed	Not allowed
Bending (θmax) only pneumatic	118 degree	137 degree
Stiffening via cables	Allowed	Allowed
Repeatability	Unsecured	Improved

5 Conclusion

In this paper we explored the possibility of introducing a different approach to the manufacturing of the I-SUPPORT soft arm through the adoption of the most inexpensive and widespread Additive Manufacturing technique namely FFF technology. A re-design of the fluidic actuators was necessary, but the AM I-SUPPORT finally demonstrated to have comparable and, in some cases, superior characteristics to cover the same task. In addition to the improvements identified in the discussion, other potential general advantages introduced with the AM approach are: scaling up or down without limitations due to the availability of basic components; the design can be easily adjusted without major implications on the manufacturing process; replacing of damaged parts is fast and straightforward. All these advantages could be of interest also for widening the impact of the soft arm on other application areas.

Funding Open access funding provided by Politecnico di Bari within the CRUI-CARE Agreement.

Compliance with ethical standards

Conflict of interest The authors declare no conflict of interests.

References

1. Stavropoulos P, Foteinopoulos P (2018) Modelling of additive manufacturing processes : a review and classification. Manuf Rev. https://doi.org/10.1051/mfreview/2017014
2. Bici M et al (2018) Development of a multifunctional panel for aerospace use through SLM additive manufacturing. Procedia CIRP 67:215–220. https://doi.org/10.1016/j.procir.2017.12.202
3. Oyesola M, Mpofu K, Mathe N (2019) A techno-economic analytical approach of laser-based additive manufacturing processes for aerospace application. Procedia Manuf 35:155–163. https://doi.org/10.1016/j.promfg.2019.05.019
4. Joshi SC, Sheikh AA (2015) 3D printing in aerospace and its long-term sustainability. Virtual Phys Prototyp 10(4):175–185. https://doi.org/10.1080/17452759.2015.1111519
5. Stano G, Di Nisio A, Lanzolla A, Percoco G (2020) Additive manufacturing and characterization of a load cell with embedded strain gauges. Precis Eng 62:113–120. https://doi.org/10.1016/j.precisioneng.2019.11.019
6. Dijkshoorn A et al (2018) Embedded sensing: Integrating sensors in 3-D printed structures. J Sensors Sens Syst 7(1):169–181. https://doi.org/10.5194/jsss-7-169-2018
7. MacDonald E et al (2014) 3D printing for the rapid prototyping of structural electronics. IEEE Access 2(July):234–242. https://doi.org/10.1109/ACCESS.2014.2311810
8. Gräbner D, Dödtmann S, Dumstorff G, Lucklum F (2018) 3-D-printed smart screw: Functionalization during additive fabrication. J Sensors Sens Syst 7(1):143–151. https://doi.org/10.5194/jsss-7-143-2018
9. Kim K, Park J, Hoon Suh J, Kim M, Jeong Y, Park I (2017) 3D printing of multiaxial force sensors using carbon nanotube (CNT)/thermoplastic polyurethane (TPU) filaments. Sensors Actuators A Phys 263:493–500. https://doi.org/10.1016/j.sna.2017.07.020
10. Coyle S, Majidi C, LeDuc P, Hsia KJ (2018) Bio-inspired soft robotics: Material selection, actuation, and design. Extrem Mech Lett 22:51–59. https://doi.org/10.1016/j.eml.2018.05.003
11. Laschi C, Mazzolai B, Cianchetti M (2016) Soft robotics: technologies and systems pushing the boundaries of robot abilities. Sci Robot 1(1):1–12. https://doi.org/10.1126/scirobotics.aah3690
12. Kim S, Laschi C, Trimmer B (2013) Soft robotics: a bioinspired evolution in robotics. Trends Biotechnol 31(5):287–294. https://doi.org/10.1016/j.tibtech.2013.03.002
13. Manti M, Cacucciolo V, Cianchetti M (2016) Stiffening in soft robotics: a review of the state of the art. IEEE Robot Autom Mag 23(3):93–106. https://doi.org/10.1109/MRA.2016.2582718
14. Lee C et al (2017) Soft robot review. Int J Control Autom Syst 15(1):3–15
15. Grzesiak A, Becker R, Verl A (2011) The bionic handling assistant: a success story of additive manufacturing. Assem Autom 31:329–333. https://doi.org/10.1108/01445151111172907
16. Gul JZ et al (2018) 3D printing for soft robotics–a review. Sci Technol Adv Mater 19(1):243–262. https://doi.org/10.1080/14686996.2018.1431862
17. Yap HK, Ng HY, Yeow CH (2016) High-Force Soft Printable Pneumatics for Soft Robotic applications. Soft Robot 3(3):144–158. https://doi.org/10.1089/soro.2016.0030
18. Keong BAW, Hua RYC (2018) A novel fold-based design approach toward printable soft robotics using flexible 3d printing materials. Adv Mater Technol 3(2):1–12. https://doi.org/10.1002/admt.201700172
19. Zhang YF et al (2019) Miniature pneumatic actuators for soft robots by high-resolution multimaterial 3D printing. Adv Mater Technol 4(10):1–9. https://doi.org/10.1002/admt.201900427
20. Ge L, Dong L, Wang D, Ge Q, Gu G (2018) A digital light processing 3D printer for fast and high-precision fabrication of soft pneumatic actuators. Sensors Actuators A Phys 273:285–292. https://doi.org/10.1016/j.sna.2018.02.041
21. Ansari Y, Manti M, Falotico E, Mollard Y, Cianchetti M, Laschi C (2017) Towards the development of a soft manipulator as an assistive robot for personal care of elderly people. Int J Adv Robot Syst 14:172988141668713. https://doi.org/10.1177/1729881416687132
22. Manti M, Pratesi A, Falotico E, Cianchetti M, Laschi C (2016) Soft assistive robot for personal care of elderly people. In: 2016 6th IEEE international conference on biomedical robotics and biomechatronics (BioRob), pp 833–838. doi: https://doi.org/10.1109/BIOROB.2016.7523731.
23. Pradel P, Zhu Z, Bibb R, Moultrie J (2018) A framework for mapping design for additive manufacturing knowledge for industrial and product design. J Eng Des 29(6):291–326. https://doi.org/10.1080/09544828.2018.1483011
24. Thompson MK et al (2016) Design for additive manufacturing: trends, opportunities, considerations, and constraints. CIRP Ann Manuf Technol 65(2):737–760. https://doi.org/10.1016/j.cirp.2016.05.004
25. Booth JW, Alperovich J, Chawla P, Ma J, Reid TN, Ramani K (2017) The design for additive manufacturing worksheet. J Mech Des Trans ASME. https://doi.org/10.1115/1.4037251
26. Khudiakova A, Arbeiter F, Spoerk M, Wolfahrt M, Godec D, Pinter G (2019) Inter-layer bonding characterisation between materials with different degrees of stiffness processed by fused filament fabrication. Addit Manuf 28(March):184–193. https://doi.org/10.1016/j.addma.2019.05.006
27. Lopes LR, Silva AF, Carneiro OS (2018) Multi-material 3D printing: The relevance of materials affinity on the boundary interface performance. Addit Manuf 23:45–52. https://doi.org/10.1016/j.addma.2018.06.027
28. Yin J, Lu C, Fu J, Huang Y, Zheng Y (2018) Interfacial bonding during multi-material fused deposition modeling (FDM) process due to inter-molecular diffusion. Mater Des 150:104–112. https://doi.org/10.1016/j.matdes.2018.04.029
29. Dey A, Yodo N (2019) A systematic survey of FDM process parameter optimization and their influence on part characteristics. J Manuf Mater Process 3(3):64. https://doi.org/10.3390/jmmp3030064
30. Mohamed OA, Masood SH, Bhowmik JL, Nikzad M, Azadmanjiri J (2016) Effect of process parameters on dynamic mechanical performance of FDM PC/ABS printed parts through design of

experiment. J Mater Eng Perform 25(7):2922–2935. https://doi.org/10.1007/s11665-016-2157-6
31. Kuznetsov VE, Solonin AN, Urzhumtsev OD, Schilling R, Tavitov AG (2018) Strength of PLA components fabricated with fused deposition technology using a desktop 3D printer as a function of geometrical parameters of the process. Polymers (Basel). https://doi.org/10.3390/polym10030313
32. Rayegani F, Onwubolu GC (2014) Fused deposition modelling (FDM) process parameter prediction and optimization using group method for data handling (GMDH) and differential evolution (DE), pp 509–519. Doi: https://doi.org/10.1007/s00170-014-5835-2.